Hindawi
Journal of Sensors
Volume 2022, Article ID 8655669, 17 pages
https://doi.org/10.1155/2022/8655669

Research Article

Prognostics and Predictive Maintenance Optimization Based on Combination BP-RBF-GRNN Neural Network Model and Proportional Hazard Model

Guoqiang Tong,[1,2] Xinbo Qian ,[1,3] and Yilai Liu[2,3]

[1]*Key Laboratory of Metallurgical Equipment and Control Technology, Ministry of Education, Wuhan University of Science and Technology, Wuhan 430081, China*
[2]*Hubei Key Laboratory of Mechanical Transmission and Manufacturing Engineering, Wuhan University of Science and Technology, Wuhan 430081, China*
[3]*Precision Manufacturing Institute, Wuhan University of Science and Technology, Wuhan 430081, China*

Correspondence should be addressed to Xinbo Qian; xinboqian@wust.edu.cn

Received 13 December 2021; Accepted 28 March 2022; Published 28 April 2022

Academic Editor: Min Xia

Owning to the advantage of keeping the operating environment safe, high reliability, and low production cost, predictive maintenance has been widely used in industry and academia. Predictive maintenance based on degeneration state mainly studies the degeneration prediction. However, on account of the error of the sensor and human, condition monitoring data may not directly reflect the true degeneration. The degeneration model with dynamic explanatory covariates which is named as proportional hazard model is proposed to deal with the semi-observed monitoring condition. And the degeneration prediction mainly adopts a single prediction model, which leads to low prediction accuracy. A combination forecasting model can effectively solve the above problem. Compared to the traditional prediction method, the neural network model can use the "black box" characteristic to indirectly construct the degeneration model without complex mathematical derivation. Therefore, we propose a combination BP-RBF-GRNN neural network model which is applied to improve the degeneration prediction with dynamic covariate. Based on the above two aspects, a predictive maintenance optimization framework based on the proportional hazard model and BP-RBF-GRNN neural network model is proposed to improve maintenance efficiency and reduce maintenance costs. The simulation results of thrust ball bearing show that the proposed method can effectively improve the degeneration prediction accuracy and reduce the maintenance cost rate to a certain extent.

1. Introduction

It can improve the reliability of equipment, greatly reduce the maintenance cost, and improve production quality, predictive maintenance (PdM) has been widely used in industry and academia [1, 2]. Engineers and researchers use condition-based monitoring data, mathematical models, and simulation to predict the degeneration process of equipment [3]. Common mathematical models or methods include artificial neural network, Bayesian network, decision tree, linear regression, principal component analysis, and random forest [4]. The data-driven method mines monitoring data to predict potential failure, which can reduce maintenance costs and improve reliability [5]. Machine learning (ML) has currently become an effective tool for PdM applications [4]. It is normally difficult to describe the physical degeneration process accurately by modeling. The neural network model can establish the mapping relationship between input and output without complex mathematical derivation. These neural networks try to replicate the way the neurons in any intelligent organism (like human neurons) are coded to take inputs. And neural networks have been used extensively for classification problems, detection problems, pattern recognition, nonlinear regression, feature

selection, time series prediction, and data normalization. In solar sunshine intensity, the BP neural network model is used to predict solar sunshine intensity [6]. In the water quality, BP neural network can be used to predict the water quality of Yuqiao Reservoir in Tianjin, and the simulation shows that the neural network has a good prediction performance on reservoir water quality [7]. In the ethanol fuel, generalized regression neural network can be used to predict the emission characteristics of ethanol fuel HCCI engine, and the results show that the error of parameter forecasting is controlled within 2% [8]. In water evaporation capacity, GRNN neural network and RBF neural network are used to estimate water evaporation capacity, respectively [9].

The core idea of PdM is to optimize maintenance policy according to some criteria, such as risk, cost, reliability, and availability. The effectiveness of this maintenance strategy is determined by the age at which PdM takes place. "Under-maintenance" will result in a high maintenance cost per unit time. "Over-maintenance" will result in a higher probability of failure and maintenance costs. The common optimization problems include the optimization of the structure, the optimization of maintenance costs, and the optimization of reliability. As for the optimization of the structure, the generalized perturbation-based Stochastic Finite Element Method can be used to optimize the structure of the truss-type [10]. As for the optimization of maintenance costs, a methodology can be proposed to minimize the life cycle maintenance costs and maximize the life cycle quality level of the track-bed [11]. As for the optimization of reliability, the mission reliability model of unmanned aerial vehicles and the measuring method can be used to support mission planning and the design of the structure [12]. The co-optimization of economy and reliability as a new target can be used to improve the reliability of energy supply [13]. A deducing-based reliability optimization method for electrical equipment can be proposed to enhance the reliability of electrical equipment [14]. The traditional method of maintenance reliability analysis includes qualitative failure mode, tree, and hazard analysis. And the common method of reliability assessment is the Bayesian approaches, reliability-based design optimization tools, multivariate analyses, and fuzzy set theory [15]. The optimization object normally includes reliability, failure rate, remaining useful life, and expected cost per unit. The expected cost per unit can normally be used as the optimization object to take maintenance activity [16].

This paper proposes a predictive maintenance optimization framework based on the proportional hazard model and BP-RBF-GRNN neural network model to improve the maintenance efficiency and reduce the maintenance cost. Owing to the accuracy of the sensor or complicated monitoring environment, the condition monitoring data may not directly reflect the degree of degeneration. Life data and condition monitoring values must be considered comprehensively. To solve the above problem, we adopt the degeneration modeling with dynamic explanatory covariates, that is, proportional hazard model (PHM), to consider both life data and condition monitoring values to evaluate the failure rate of mechanical equipment. Compared with the traditional conditional variable or basic reliability model, PHM can reflect the statistical characteristics of the whole sample to reduce the error of failure rate evaluation. In addition, the single prediction model can easily lead to low accuracy, and we adopt the combination BP-RBF-GRNN neural network model to improve the prediction performance. The reason for the choice of sub-prediction model is as follows. The BP neural network model has high prediction accuracy, but it easily falls down the local minimum and has a slow convergence speed. RBF neural network model can solve the problem of local minimum caused by BP, but it has a low prediction accuracy when there are few data samples. The GRNN neural network model has good generalization ability and is good at dealing with prediction under small samples. Therefore, this paper uses a combination forecasting model which contains BP, RBF, and GRNN neural network to predict the degeneration process.

The structure of this paper is as follows. Section 2 is the degeneration model with dynamic covariates. Section 3 is the degeneration prognostics based on covariates prediction via combination BP-RBF-GRNN neural network model. Section 4 is predictive maintenance optimization based on degeneration prognosis. Section 5 is the simulation case study. Section 6 is the conclusion.

2. Degeneration Modeling with Dynamic Covariates

In industrial applications, the risk factor which is called covariate affects the lifetime of the mechanical equipment, and it may influence or indicate the failure time. The covariates can be classified into external and internal variables [17]. The external covariate changes over time, but it is not affected by previous failure. The internal covariate is the measurement of the individual, and it is affected by survival state. As for the research of prognostics and life prediction, probabilistic model using covariates that contains the diagnostic factors and operating environment factors has become one of the indispensable methods [18]. The proportional hazard model is one of the basic theories of the covariate model, which uses the historical failure data to build the baseline hazard function and uses covariate data to build the covariate function.

The hazard rate of WPHM contains the baseline failure rate function and an exponential function including the effect of the monitoring variable, as shown in Equation (1).

$$h(t) = h_0(t) \exp(\gamma_i Z_i), \tag{1}$$

where the baseline hazard rate $h_0(t)$ is related to the historical lifetime, and the covariate Z_i is a row vector of the monitoring variable at the time t. The covariance coefficient γ_i is a column vector corresponding to the i_{th} monitoring variable.

The baseline failure rate function is shown in Equation (2).

$$h_0(t) = \frac{\beta}{\eta}\left(\frac{t}{\eta}\right)^{\beta-1}, \tag{2}$$

where β is the shape parameter and η is the scale parameter.

According to the principle of reliability analysis, the reliability and failure probability density function can be obtained by Equation (3).

$$R(t) = \exp\left[-\int_0^t h(t)dt\right]. \tag{3}$$

The maximum likelihood method is constructed to estimate the unknown parameters of WPHM. As shown in Equation (4), the likelihood function is as follows.

$$L(\beta, \eta, \gamma) = \prod_{i=1}^{n} f(t_i) \prod_{j=1}^{m} R(t_i), \tag{4}$$

where n is the number of failure samples and m is the number of suspension samples.

The optimal solution of the parameters can be obtained by solving the partial derivatives of Equation (5).

$$L(\beta, \eta, \gamma) = \prod_{i=1}^{n} \frac{\beta}{\eta}\left(\frac{t_i}{\eta}\right)^{\beta-1} \exp\left(\gamma Z_{t_i}\right) \prod_{j=1}^{n+m} \exp\left[-\left(\frac{t_j}{\eta}\right)^{\beta} \exp\left(\gamma Z_{t_j}\right) dt\right]. \tag{5}$$

Since the condition monitoring data measured by the various sensors can partially reflect the actual degeneration state, the monitoring data can be regarded as dynamic covariates to build a degeneration model. The degeneration model based on monitoring data is as follows [19]. We assume that $Z_i(t_{ij})$ can be the observed condition monitoring measurements for the unit i at the time t_{ij}, where $i = 1, \cdots, n$, $j = 1, \cdots, m$, n is the number of units, and m is the number of measurement points for unit i. $Z_i(t) = [Z_{i1}(t), \cdots, Z_{ik}(t)]$ is a vector of dynamic covariate observation, where $k = 1, \cdots, p$, and p is the number of the dynamic covariate. Therefore, $Z_i(t) = \{Z_i(T), 0 \le T \le t\}$ represents the history of dynamic covariate process for unit i at time t. In conclusion, $Z(t) = \{Z_1(t), \cdots, Z_n(t)\}$ is the history of the dynamic covariate process from time 0 to time t for all units n.

3. Degeneration Prognostics Based on Covariates Prediction via Combination BP-RBF-GRNN Neural Network Model

3.1. Prediction Sub-Model

3.1.1. BP Neural Network. As shown in Figure 1, the back-propagation (BP) neural network is a feed-forward neural network, which is one of the common neural networks and has good learning ability. The learning rule is to constantly adjust the weight and threshold of network connection by the steepest descent method [20]. But the method of obtaining the optimal parameters with the gradient descent can easily fall into local minimum [21].

The training process of BP neural network is as follows [22, 23].

Step 1. Initialize parameters of BP network.

It is needed to confirm the weight, the threshold, and the number of neurons in each layer.

Step 2. Calculate the j_{th} neuron of output H in the hidden layer.

$$H_j = f\left(\sum_{i=1}^{n} w_{ij} X_i - a_j\right), \tag{6}$$

where $X = [X_1, \cdots, X_i, \cdots, X_n]'$ is a input matrix, $i = 1, 2, 3, \cdots, n$, n is the length of time series for the covariate, and it is also the number of input layer neurons. $X_i = [x_1, \cdots, x_{s_1}]$ represents the monitoring value of covariate at time i for all samples s_1. $j = 1, 2, \cdots, g$, g is the number of neurons in the hidden layer. $O = [O_1, \cdots, O_k, \cdots, O_m]'$ is an output matrix, $k = 1, 2, 3, \cdots, m$, m is the length of time series for the covariate, and it is also the number of output layer neurons. $O_k = [o_1, \cdots, o_{s_2}]$ represents the predicted value of covariate at time k for all samples s_2.

Step 3. Calculate the k_{th} neuron of output O in the output layer.

$$O_k = f\left(\sum_{j=1}^{l} H_j w_{jk} - b_k\right). \tag{7}$$

Step 4. Calculate the error E.

$$E = \frac{1}{2}\sum_{k=1}^{m} (Y_k - O_k)^2, \tag{8}$$

where O_k is the predictive result and Y_k is the expected output.

Step 5. Update the weight w.

The weight and threshold of the network should be modified along the negative gradient direction with the fastest function decline.

The weight w_{jk} is updated by Equation (9).

$$w_{jk} = w_{jk} + \eta H_j e_k, \tag{9}$$

where η is the learning rate.

The weight w_{ij} is updated by Equation (10).

$$w_{ij} = w_{ij} + \eta' \left(1 - H_j^2\right) X(i) \sum_{k=1}^{m} w_{jk} e_k, \tag{10}$$

where η' is the learning rate.

Step 6. Update the threshold values a and b.

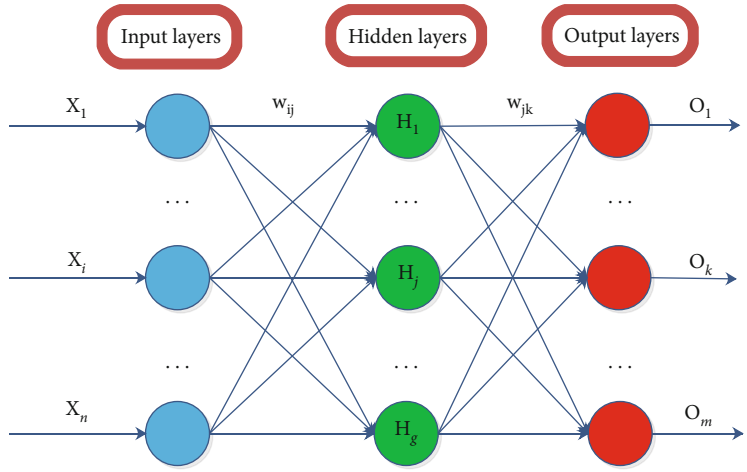

Figure 1: The architecture of BP neural network.

The process of updating the threshold is similar to the process of updating weight. The process of updating the threshold values a and b is as follows.

$$b_k = b_k + \eta e_k, \tag{11}$$

$$a_j = a_j + \eta' \left(1 - H_j^2\right) \sum_{k=1}^{m} w_{jk} e_k. \tag{12}$$

Step 7. Determine the requirement of iteration.

If the iteration requirement is not met, it should repeat the process from Step 2 to Step 6. Otherwise, trained neural network parameters can be outputted.

3.1.2. RBF Neural Network. As shown in Figure 2, the radial basis function (RBF) is a two-layer feed-forward network with a single hidden layer [24], which can approximate the nonlinear function with arbitrary precision and realize the global optimization in theory [25]. It is a direct mapping from the input layer to the hidden layer. Therefore, the training time of parameters is shorter than BP neural network. The hidden layer and output layer are connected by the linear weight.

As shown in Equation (13), the radial basis function is used as the node transfer function of the hidden layer.

$$R_j = \exp\left[\frac{(X - c_j)^T (X - c_j)}{2\sigma_j^2}\right], \tag{13}$$

where $X = [X_1, \cdots, X_i, \cdots, X_n]'$ is a input matrix, $i = 1, 2, 3, \cdots, n$, n is the length of time series for the covariate, and it is also the number of input layer neurons. $X_i = [x_1, \cdots, x_{s_1}]$ represents the monitoring value of covariate at time i for all samples s_1. R_j is the output of the j_{th} hidden node, c_j is the center of the Gaussian function in the j_{th} hidden node, σ_j is the output standardized variance of the j_{th} hidden node, $j = 1, 2, \cdots, g$, and g is the number of neurons in the hidden layer. $O = [O_1, \cdots, O_k, \cdots, O_m]'$ is an output matrix, $k = 1, 2, 3, \cdots, m$, m is the length of time series for the covariate, and it is also the number of output layer neurons. $O_k = [o_1, \cdots, o_{s_2}]$ represents the predicted value of covariate at time k for all samples s_2.

The k_{th} neuron output O_k in the output layer is shown in Equation (14).

$$O_k = \sum_{j=1}^{l} w_{jk} \bullet R_j, \tag{14}$$

where l is the number of neurons in the hidden layer, $k = 1, 2, 3, \cdots, m$, and m is the number of neurons.

3.1.3. GRNN Neural Network. As shown in Figure 3, generalized regression neural network (GRNN) has four layers. GRNN is also a kind of radial basis function neural network [26], which is used to solve the regression problem. It has more advantages than RBF neural network in approximation ability and learning speed. Especially, it has a good effect in prediction under small samples.

Data transmission from the input layer to the pattern layer is direct transmission. In the pattern layer, the transfer function is the radial basis function, as shown in Equation (15).

$$P_i = \exp\left[-\frac{(X - X_i)^T (X - X_i)}{2\sigma^2}\right], \tag{15}$$

where $X = [X_1, \cdots, X_i, \cdots, X_n]'$ is a input matrix, $i = 1, 2, 3, \cdots, n$, n is the length of time- series for the covariate, and it is also the number of input layer neurons. $X_i = [x_1, \cdots, x_{s_1}]$ represents the monitoring value of covariate at time i for all samples s_1. P_i is the output of the i_{th} hidden node; σ denotes the smoothing parameter. S_D is the first type of the summation; S_N is the second type of the summation. $O = [O_1, \cdots, O_k, \cdots, O_m]'$ is an output matrix, $k = 1, 2, 3, \cdots, m$, m is the length of time series for the covariate, and it is also the number of output layer neurons. $O_k = [o_1, \cdots, o_{s_2}]$

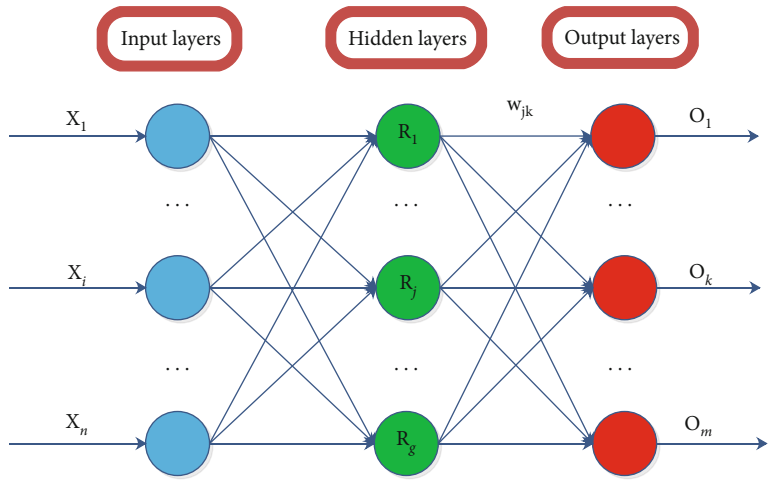

Figure 2: The architecture of RBF neural network.

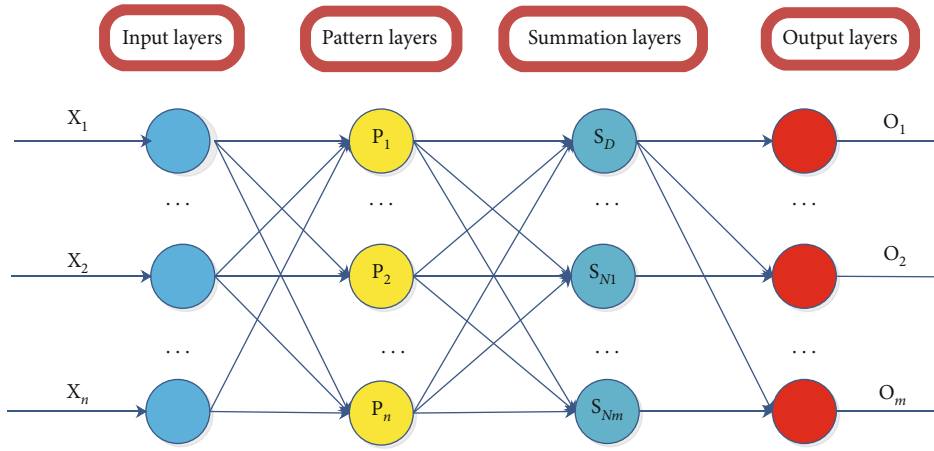

Figure 3: The architecture of GRNN neural network.

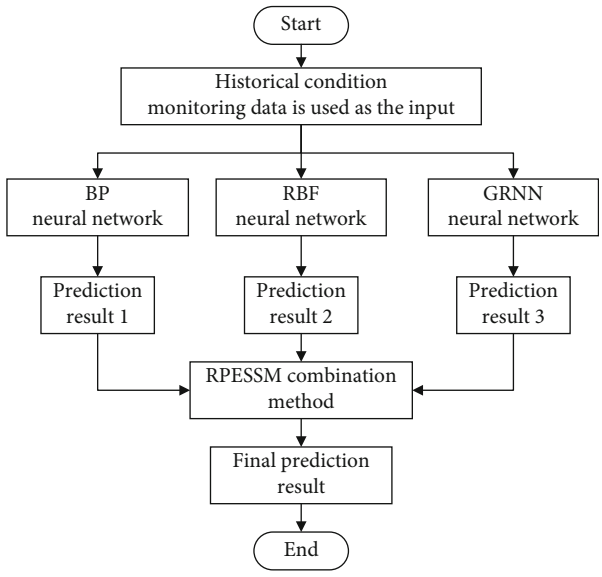

Figure 4: Flow chart of the combination forecasting method.

represents the predicted value of covariate at time k for all samples s_2.

There are two summations in the summation layer [27], namely, S_D and S_{NK}.

The first type of summation is shown in Equation (16).

$$S_D = \sum_{i=1}^{n} P_i. \tag{16}$$

The second type of summation is shown in Equation (17).

$$S_{Nk} = \sum_{i=1}^{n} w_{ik} P_i. \tag{17}$$

The output layer can be calculated as shown in Equation (21).

$$O_k = \frac{S_{Nk}}{S_D}. \tag{18}$$

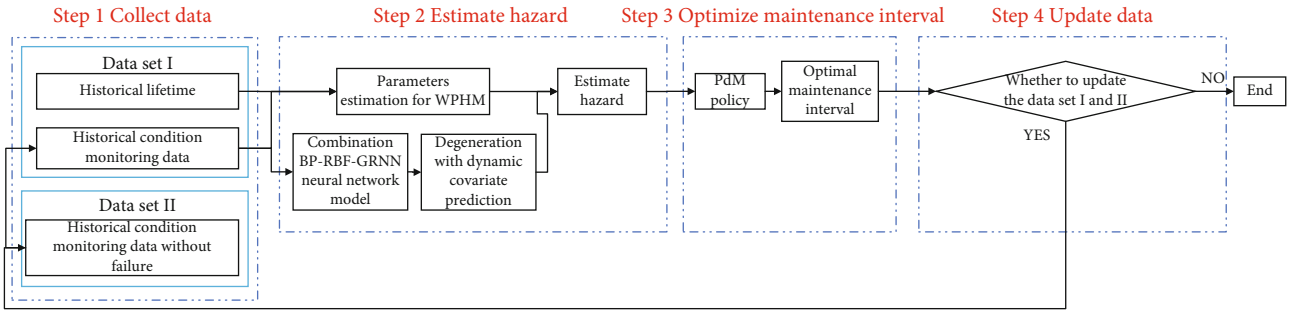

Figure 5: Flow chart of the PdM model framework based on combination BP-RBF-GRNN neural network model and proportional hazard model.

Table 1: Parameter distribution of covariate model.

Symbol	Normal distribution	Numerical value
μ_0	Mean	-6.031
σ_0^2	Variance	0.346
μ_1	Mean	8.061×10^{-3}
σ_1^2	Variance	1.034×10^{-5}
μ	Mean	0
σ^2	Variance	7.3×10^{-3}

3.2. Combination Method. As shown in Figure 4, three prediction sub-models, respectively, use historical monitoring data to predict the degeneration process, and the final prediction result will be output by the combination method. The combination forecasting model makes use of the characteristics of different sub-models to comprehensively improve the prediction performance. Reciprocal prediction error sum of squares method (RPESSM) can be used as the combination method to predict degeneration process [28, 29]. A small RPESSM value indicates the high performance of the prediction sub-model.

Therefore, y_{1t}, y_{2t}, and y_{3t} show the prediction result of the BP, RBF, and GRNN neural network at the time t, respectively. And e_{1t}, e_{2t}, and e_{3t} are the prediction errors correspondingly. As shown in Equation (19), y_t is the prediction result of the combination BP-RBF-GRNN neural network model at the time t, respectively. As shown in Equations (20) to (22), w_{1t}, w_{2t}, and w_{3t} are the weight coefficients at the time t.

$$\begin{cases} y_t = w_{1t} \bullet y_{1t} + w_{1t} \bullet y_{1t} + w_{1t} \bullet y_{1t} \\ w_{1t} + w_{2t} + w_{3t} = 1 \end{cases}, \tag{19}$$

$$w_{1t} = \frac{e_{1t}^2}{e_{1t}^2 + e_{2t}^2 + e_{3t}^2}, \tag{20}$$

$$w_{2t} = \frac{e_{2t}^2}{e_{1t}^2 + e_{2t}^2 + e_{3t}^2}, \tag{21}$$

$$w_{3t} = \frac{e_{3t}^2}{e_{1t}^2 + e_{2t}^2 + e_{3t}^2}. \tag{22}$$

The role of the weight coefficient allocation is to make prediction sub-model with the highest prediction accuracy play a decisive role in the final prediction result, thus reducing the negative influence of other prediction sub-models. Therefore, the combination forecasting model can overcome the low prediction accuracy of the single prediction sub-model.

4. Predictive Maintenance Optimization Based on Degeneration Prognosis

4.1. The Framework of Predictive Maintenance Optimization. As shown in Figure 5, a PdM optimization framework based on the combination BP-RBF-GRNN neural network model and proportional hazard model is proposed in this section. The first step is to collect historical lifetime and condition monitoring data, which can be divided into two types. Data set I containing historical lifetime and historical condition monitoring data is used as the input of the WPHM and combination BP-RBF-GRNN neural network model for parameter estimation. Data set II containing historical condition monitoring data without failure is used for the performance evaluation of condition forecasting. In the second step, the hazard can be predicted based on both condition forecasting and WPHM. In the third step, the optimal preventive maintenance interval is updated by the PdM policy. At the last step, the optimal maintenance interval will be updated with the updated condition monitoring data and events.

4.2. Predictive Maintenance Optimization Policy Based on Proportional Hazard Model. As shown in Equation (23), a quantitative function of the average cost in a maintenance period for PdM optimization policy is established, which is named as the cost rate function. The PdM policy for the optimal age replacement can be divided into two types [30]. One is to reach the replacement life T under the condition of preventive maintenance, and the other is to reach the actual lifetime τ under the condition of repairing upon failure. Therefore, the cost types can be divided into two categories correspondingly. C_{PM} denotes the cost of preventive maintenance at the maintenance life T and C_{ER} denotes

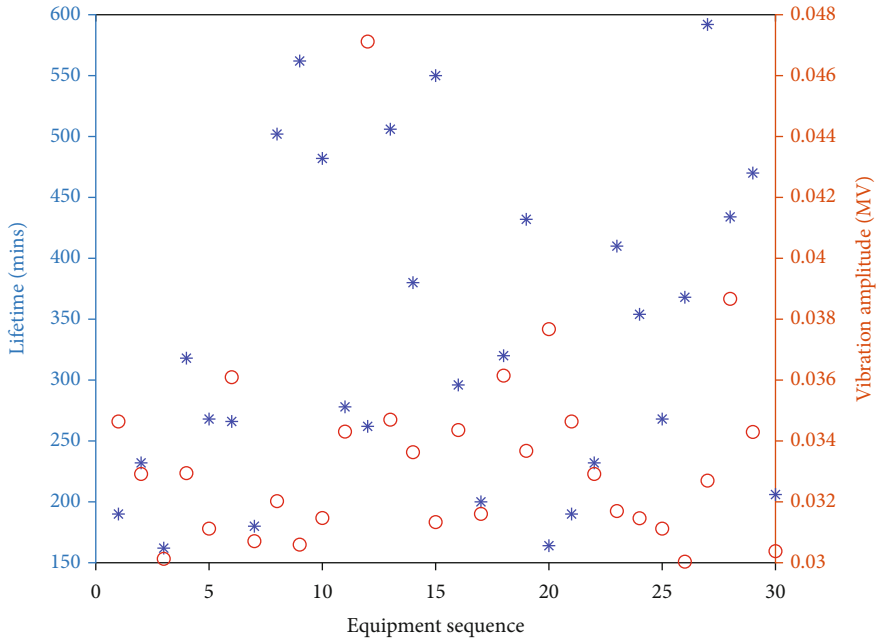

Figure 6: Lifetime data and vibration amplitude of thrust ball bearings.

Table 2: Combination scheme of training set and test set.

Training set	Test set
#2, #3, #4, #5, ⋯, #30	#1
#1, #3, #4, #5, ⋯, #30	#2
#1, #2, #4, #5, ⋯, #30	#3
#1, #2, #3, #5, ⋯, #30	#4
...	...
#1, #2, #3, #4, ⋯, #29	#30

the cost of corrective maintenance at the maintenance life τ. In general, C_{ER} is greater than C_{PM}.

$$\eta_{\text{age}}(T) = \min_{T} \frac{F(T)C_{ER} + (1 - F(T))C_{PM}}{\int_0^T (1 - F(X))dx}, \tag{23}$$

where the denominator is the average maintenance age, and the numerator is the average maintenance cost in a period. $F(t)$ is the unreliability function which can be obtained by the Weibull distribution proportional hazard model. Owning to the difficult explicit expression by the form of the mathematical formula, it is hard to solve the optimal solution. Therefore, an approximate solution method, namely, the trapezoidal numerical integration method, is used to solve the calculation problem.

5. Simulation Case Study

5.1. Prediction Performance Criteria. The evaluation index of prediction performance adopts root mean square percentage error (RMSPE) and root mean square error (RMSE) [31].

$$\text{RMSPE} = \sqrt{\frac{1}{N}\sum_{i=1}^{N}\left(\frac{y_{i-}\widehat{y}_i}{y_i}\right)^2} \times 100\%, \tag{24}$$

$$\text{RMSE} = \sqrt{\frac{1}{N}\sum_{i=1}^{N}(y_{i-}\widehat{y}_i)^2}, \tag{25}$$

where y_i is the actual value, $\widehat{y}_i$ is the prediction, and N is the length of time series. RMSPE is a relative error-index, which shows the deviation between the prediction and the actual value. RMSE reflects the dispersion and concentration of error size and distribution.

5.2. Maintenance Performance Criteria. To measure the maintenance performance between combination BP-RBF-GRNN neural network model and the traditional prediction model (Bayesian parameter updating prediction model) in PdM policy, we establish the evaluation index, as shown in Equations (26) and (27) [32].

$$R^i_{T\text{opt}} = \left(\frac{T\text{opt}^i_C}{T\text{opt}^i_P} - 1\right) \times 100\%, \tag{26}$$

where T_{opt} is the optimal maintenance interval. And the letters subscript of "P" indicates the prediction model to be compared, and the letters subscript of "C" indicates the combination BP-RBF-GRNN neural network model. $R^i_{T\text{opt}}$

Table 3: Model parameters of BP neural network.

The parameter name	Value or option
P	Input matrix. $(tk/2) \times 29$
T	Output matrix. $(t\text{end} - tk/2) \times 1$
Hidden layer nodes (S)	18
Hidden layer nodes transfer function type (TF)	tansig
Output layer neuron transfer function type (TF)	logsig
Training function type (BTF)	traingd
Learning function type (BLF)	learngdm
The max iteration number	7000
Network training goal error	0.01

Table 4: Model parameters of RBF neural network.

The parameter name	Value or option
P	Input matrix. $(tk/2) \times 29$
T	Output matrix. $(t\text{end} - tk/2) \times 1$
Network training goal error	0.001
Spread of radial basis function	0.01
Maximum number of neurons (MN)	400
Number of neurons to add between displays (DF)	5

Table 5: Model parameters of GRNN neural network.

The parameter name	Value or option
P	Input matrix. $(tk/2) \times 29$
T	Output matrix. $(t\text{end} - tk/2) \times 1$
Spread of radial basis function	0.01

represents the relative error percentage in maintenance interval under the i_{th} training-test set scheme.

$$R_{\eta}^{i} = \left(\frac{\eta_{C}^{i}\left(\text{Topt}_{P}^{i}\right)}{\eta_{C}^{i}\left(\text{Topt}_{C}^{i}\right)} - 1 \right) \times 100\%, \tag{27}$$

where η is the minimum cost rate under the optimal maintenance age. And R_{η}^{i} represents the relative error percentage in cost rate the i_{th} training-test set scheme.

5.3. Case Study

5.3.1. Data Sources. As shown in Equation (28) [33], we use the popular covariate model of vibration degeneration by the MATLAB software for the simulation [34]. Equation (29) can be obtained by the logarithm of Equation (36). Table 1 shows the probability distributions of model parameters in Equation (29) [35].

$$S(t) = \varnothing + \theta \exp\left(\beta t + \varepsilon(t) - \frac{\sigma^2}{2} t\right), \tag{28}$$

$$L(t) = \ln\left(S(t) - \varnothing\right) = \theta' + \beta' + \varepsilon(t), \tag{29}$$

where $\theta' \sim N(\mu_0, \sigma_0^2)$, $\beta' \sim N(\mu_1', \sigma_1^2)$, and $\varepsilon(t_i) - \varepsilon(t_{i-1}) \sim N(\mu, \sigma^2)$). $\varepsilon(t)$ follows winner process, and it can be generated by the method of pseudo-random number. Simulation failure threshold is D=0.03 MV [33], simulation length is 600 minutes, and simulation interval is 2 minutes. And we generate 30 group thrust ball bearing vibration signals for the simulation case study. The double ordination of the simulation lifetime data and simulation vibration amplitude is shown in Figure 6.

5.3.2. Experiment Design. As shown in Table 2, to avoid the problem of overfitting, we designed the experiment by the method of leave-one-out cross-validation, and chose 1 group as the test set and another 29 groups as the training set. Therefore, there are 30 training-test set schemes.

We focus on five prediction point values of t_{ki}, $t_{ki} \in \{0.1T_{Aj}, 0.3T_{Aj}, 0.5T_{Aj}, 0.7T_{Aj}, 0.9T_{Aj}\}$, which represent the early-stage, early-to-mid stage, mid-stage, mid-to-late stage, and late-stage for each component j, respectively. T_{Aj} is the actual life of component j. As shown in Equations (30)–(32), we use the modified newff MATLAB toolbox to construct the structure of the BP neural network, use the newrb MATLAB toolbox to construct the structure of the RBF neural network, and use the newgrnn MATLAB toolbox to construct the structure of GRNN neural network. And the detailed parameters are determined as shown in Tables 3–5.

$$\text{net} = \text{newff}(\text{P}, \text{T}, \text{S}, \text{TF}, \text{BTF}, \text{BLF}), \tag{30}$$

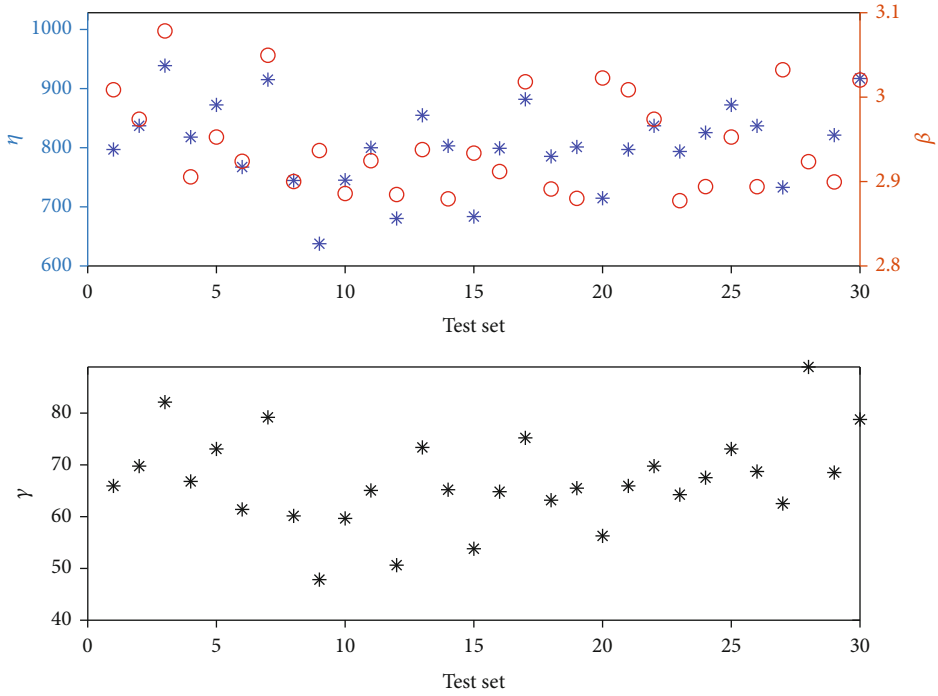

Figure 7: WPHM parameters.

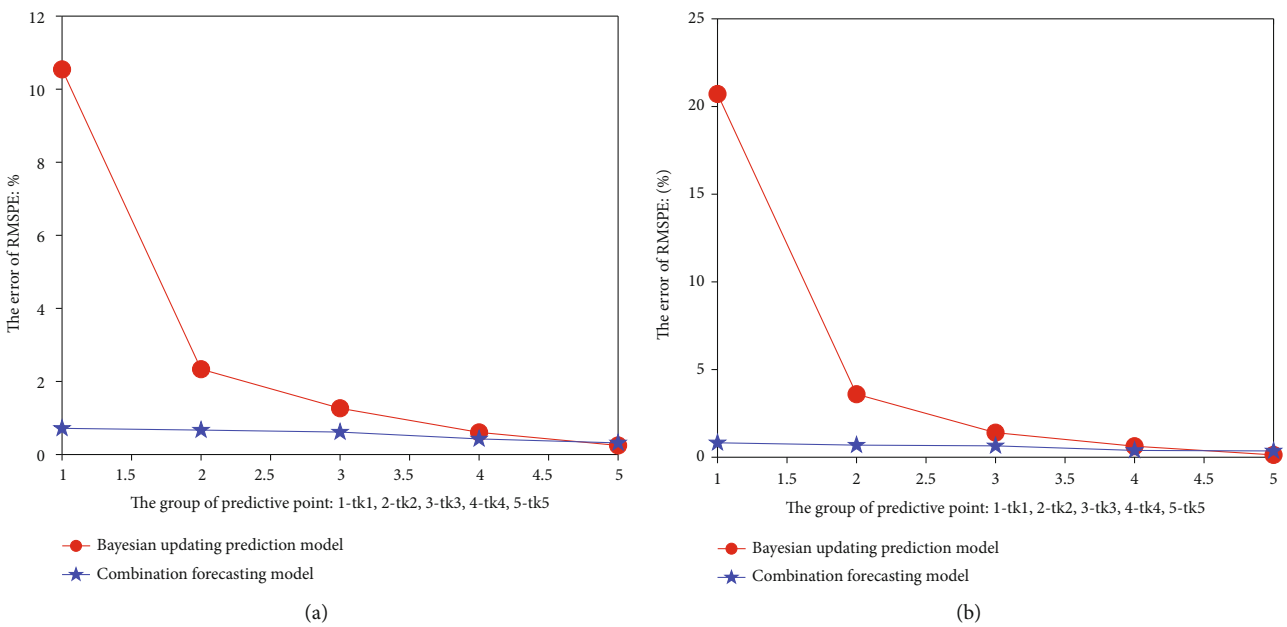

Figure 8: The error of RMSPE. (a) RMSPE mean; (b) RMSPE standard deviation.

$$\text{net} = \text{newrb}(\text{P}, \text{T}, \text{goal}, \text{spread}, \text{MN}, \text{DF}), \quad (31)$$

$$\text{net} = \text{newgrnn}(\text{P}, \text{T}, \text{spread}). \quad (32)$$

Where t_k is the prediction start point, t_{end} is the prediction end point, and sample interval is 2 minutes. We take 29 samples of $[0, t_k]$ time series monitoring data as the input vector and 1 sample of $[t_k, t_{\text{end}}]$ time series monitoring data as the output vector. Where tansig means hyperbolic tangent sigmoid transfer function, logsig means log-sigmoid transfer function, traingd means gradient descent backpropagation, learngdm means gradient descent with momentum weight and bias learning function.

5.3.3. Result Analysis. The main WPHM parameters under 30 training-test set schemes, i.e., the covariance coefficient γ, the shape parameter β, and the scale parameter η, are shown in Figure 7.

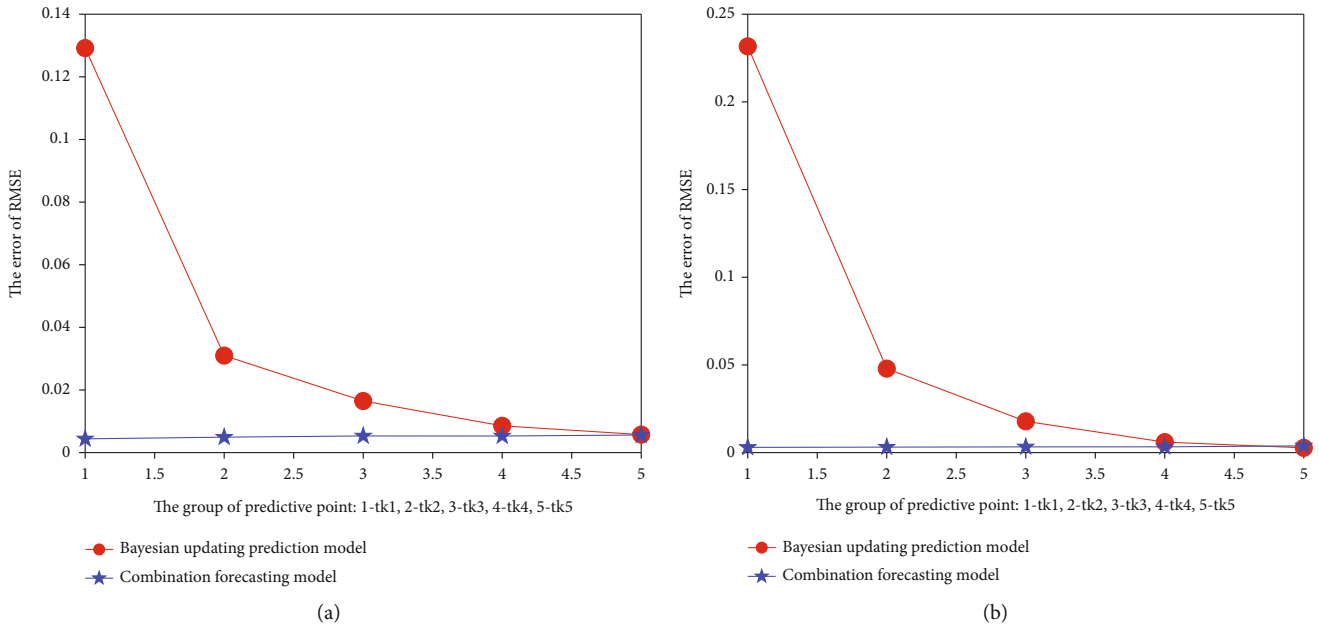

Figure 9: The error of RMSE. (a) RMSE mean; (b) RMSE standard deviation.

Figure 8 shows the mean and standard deviation of RMSPE under 30 training-test set schemes, respectively. Figure 9 shows the mean and standard deviation of the RMSE under 30 training-test set schemes, respectively. We can draw two conclusions. One is that the prediction accuracy of the Bayesian parameter updating prediction model and combination BP-RBF-GRNN neural network model can be improved when the prediction point shifts right. The other is that the prediction accuracy of the combination BP-RBF-GRNN neural network model is higher than that of the Bayesian parameter updating prediction model from the early-stage to mid-stage. But the prediction accuracy of two prediction models is nearly equivalent from mid-to-late stage to late-stage.

Figure 10 shows the box diagram of the cost ratio percentage when $C_{PM}/C_{ER} = 0.3$, $C_{PM}/C_{ER} = 0.2$, and $C_{PM}/C_{ER} = 0.1$. Figure 11 shows the box diagram of the maintenance interval percentage when $C_{PM}/C_{ER} = 0.3$, $C_{PM}/C_{ER} = 0.2$, and $C_{PM}/C_{ER} = 0.1$. Figure 12(a) shows the average cost rate percentage with three maintenance ratios under 30 training-test set schemes. Figure 12(b) shows the average maintenance interval percentage with three maintenance ratios under 30 training-test set schemes. Figure 12 shows that the maintenance ratio has a great influence on the average cost percentage and the average maintenance interval percentage from the early-stage to mid-stage. With the increasement of maintenance cost ratio (C_{PM}/C_{ER}), the combination BP-RBF-GRNN neural network model has more advantages than the Bayesian parameter updating prediction model in cost rate percentage and maintenance interval percentage from the early-stage to mid-stage.

To validate the effectiveness of the combination BP-RBF-GRNN neural network model, we have compared the combination BP-RBF-GRNN neural network model to other three single deep learning models which are named the BP, RBF, and GRNN neural network models in prediction performance and maintenance performance. The leave-one-out cross-validation is used as the validation method. The model parameters of the combination BP-RBF-GRNN neural network model are shown in Tables 3–5. RMSE is used as the prediction performance criteria.

Tables 6–8, respectively, show the maintenance performance comparison of cost rate percentage between the single deep learning model and combination BP-RBF-GRNN neural network model. As shown in (27), the cost rate percentage of Tables 6–8 uses the cost of BP, RBF, and GRNN neural network model to be divided by that of the combination BP-RBF-GRNN neural network model, respectively. The value of cost rate percentage in Tables 6–8 is greater than 0, which means that the cost of other three single deep learning models is higher than that of the combination BP-RBF-GRNN neural network model. And if the value of the cost rate percentage is high, the cost of the combination BP-RBF-GRNN neural network model will be low. Tables 9–11, respectively, show the maintenance performance comparison of maintenance interval percentage between the single deep learning model and combination BP-RBF-GRNN neural network model. As shown in (26), the maintenance interval percentage of Tables 9–11 uses the maintenance interval of the combination BP-RBF-GRNN neural network model to be divided by that of the BP, RBF, and GRNN neural network model, respectively. The value of maintenance interval percentage in Tables 9–11 is greater than 0, which means that the maintenance performance of the combination BP-RBF-GRNN neural network model is higher than that of other three single deep

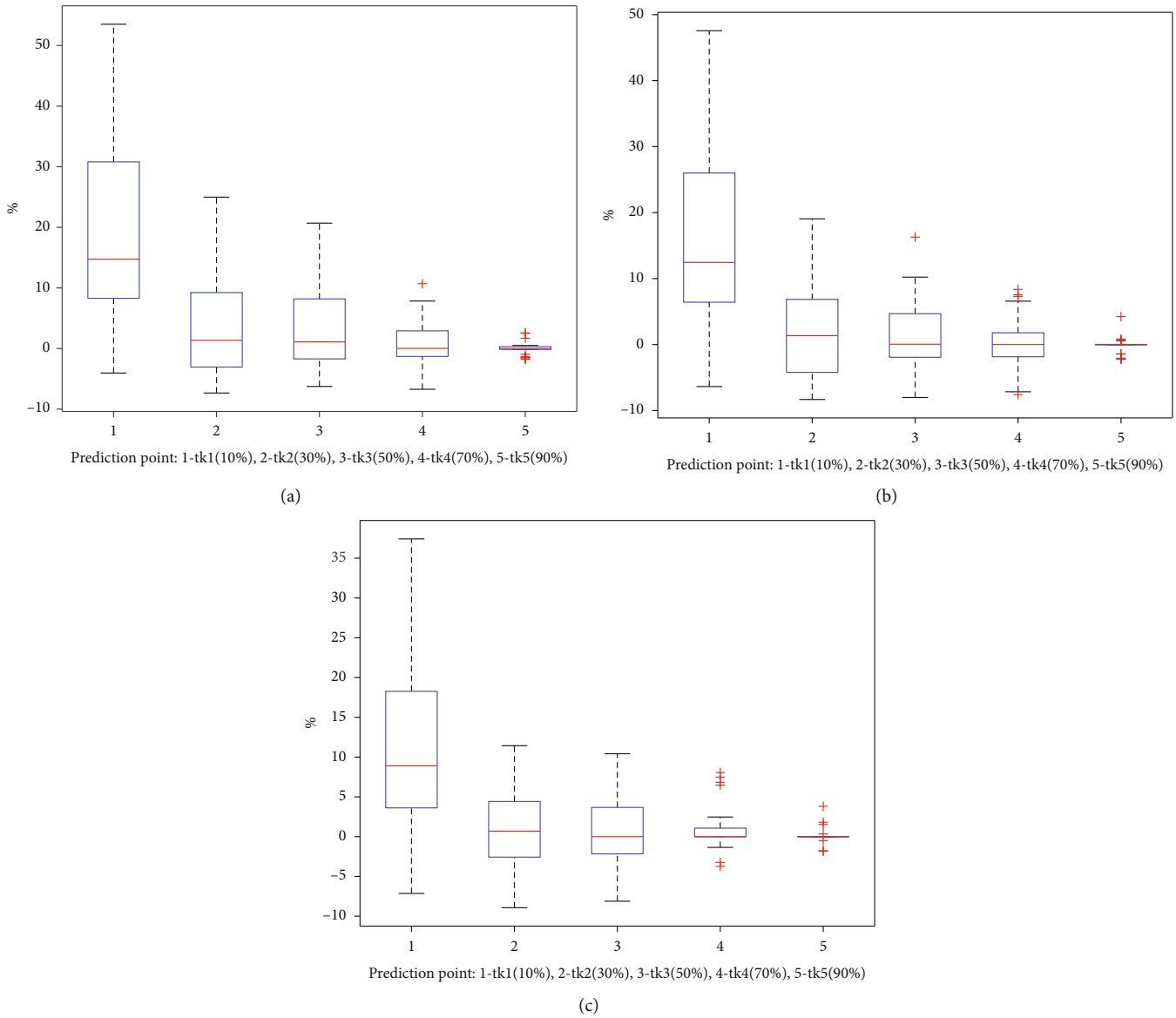

FIGURE 10: Box diagram of cost rate percentage. (a) Box diagram of cost rate percentage when $C_{PM}/C_{ER} = 0.3$. (b) Box diagram of cost rate percentage when $C_{PM}/C_{ER} = 0.2$. (c) Box diagram of cost rate percentage when $C_{PM}/C_{ER} = 0.1$.

learning models. And if the value of the maintenance interval percentage is high, the maintenance performance of the combination BP-RBF-GRNN neural network model will be good. Table 12 shows the prediction performance comparison of the BP, RBF, GRNN, and combination BP-RBF-GRNN neural network model. Tables 6 and 9 indicate that the cost rate percentage and maintenance interval percentage of the combination BP-RBF-GRNN neural network model from the early-stage to the mid-stage are more advantageous than that of BP. And with the increasement of maintenance cost ratio, the combination BP-RBF-GRNN neural network model has advantages over the BP in cost rate percentage and maintenance interval percentage. Table 7 indicates that the cost rate percentage of the combination BP-RBF-GRNN neural network model is basically equivalent to that of RBF. Table 10 indicates that the maintenance interval percentage of the combination BP-RBF-GRNN neural network model from the early-stage to the mid-to-late stage is more advantageous than that of RBF. And with the increasement of maintenance cost ratio, the combination BP-RBF-GRNN neural network model has advantages over the RBF in cost rate percentage and maintenance interval percentage. Tables 8 and 11 indicate that the cost rate percentage and maintenance interval percentage of the combination BP-RBF-GRNN neural network model from the early-stage to the mid-stage are more advantageous than those of GRNN. And with the increasement of maintenance rate, the combination BP-RBF-GRNN neural network model is basically equivalent to the GRNN in cost rate percentage and maintenance interval percentage. Table 12 indicates that the prediction accuracy of BP and GRNN can be improved with the predicted point moving right. And RBF

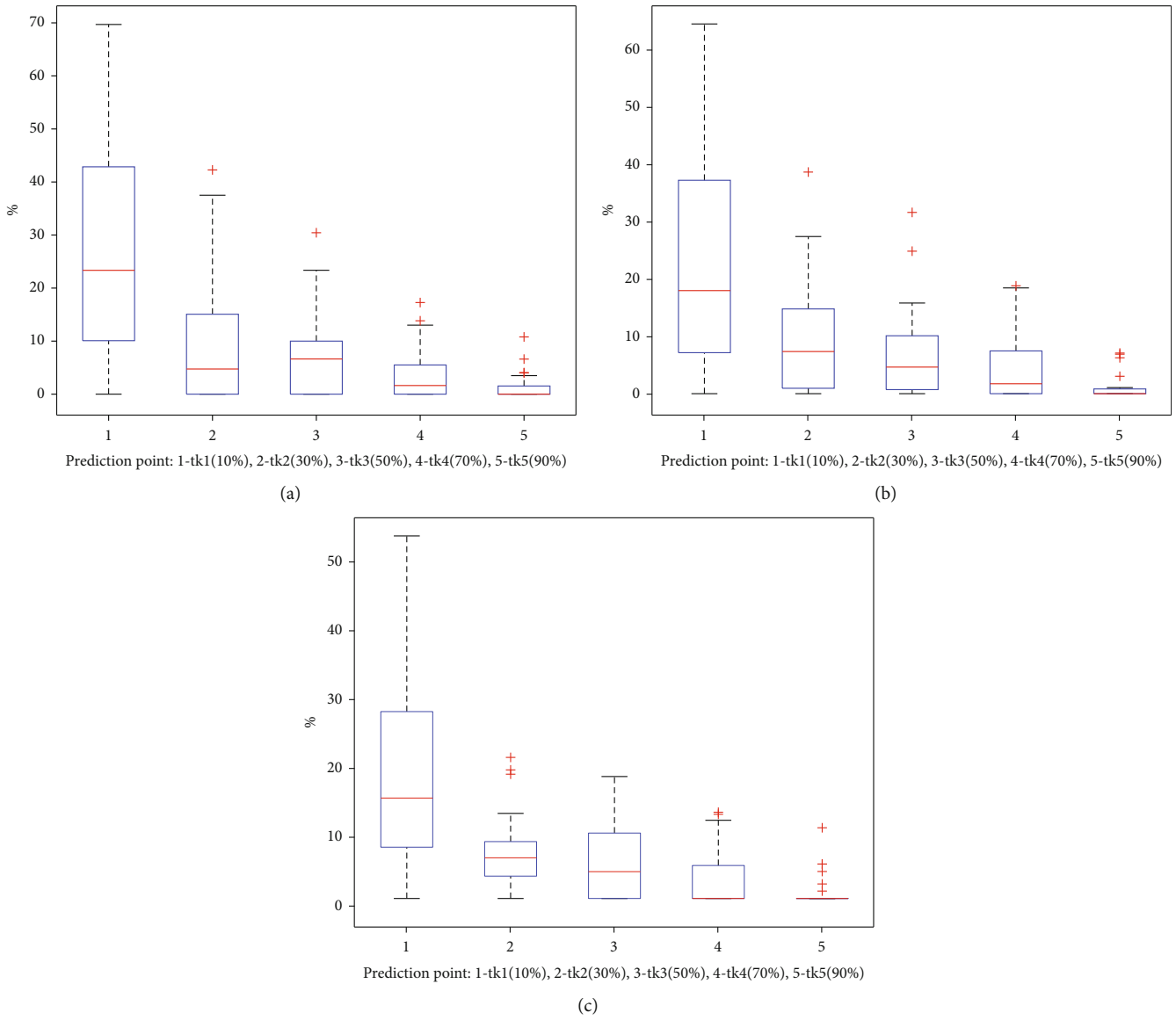

Figure 11: Box diagram of maintenance interval percentage. (a) Box diagram of maintenance interval percentage when $C_{PM}/C_{ER} = 0.3$. (b) Box diagram of maintenance interval percentage when $C_{PM}/C_{ER} = 0.2$. (c) Box diagram of maintenance interval percentage when $C_{PM}/C_{ER} = 0.1$.

can control the prediction error at a relatively stable range. It is obvious to find that the prediction accuracy of combination BP-RBF-GRNN neural network model is higher than that of the BP, RBF, and GRNN under five prediction points.

To justify the validity of the proposed method, we will change the covariate simulation parameters to simulate the other degeneration scenarios, and verify the proposed method. The covariate model parameters of θ' and β' are the original property of thrust ball bearing vibration, and the covariate model is mainly affected by the error term $\varepsilon(t)$ which represents the noise in the operation environment or the measurement error caused by the human. Moreover, the high value of the error term $\varepsilon(t)$ will increase the degeneration degree of thrust ball bearing, and lead to the decline of lifetime. Therefore, as shown in Table 13, we designed three simulation experiments by changing the normal distribution of error term $\varepsilon(t)$ to randomly simulate the different degeneration scenarios, and test the prediction performance and maintenance performance of the combination BP-RBF-GRNN neural network model. Each simulation experiment will generate 30 group thrust ball bearing vibration signals to be used as data sources. And we focus on five prediction point values of t_{ki}, $t_{ki} \in \{0.1T_{Aj}, 0.3T_{Aj}, 0.5T_{Aj}, 0.7T_{Aj}, 0.9T_{Aj}\}$, which represent the early-stage, early-to-mid stage, mid-stage, mid-to-late stage, and late-stage for each component j, respectively. T_{Aj} is the actual life of component j.

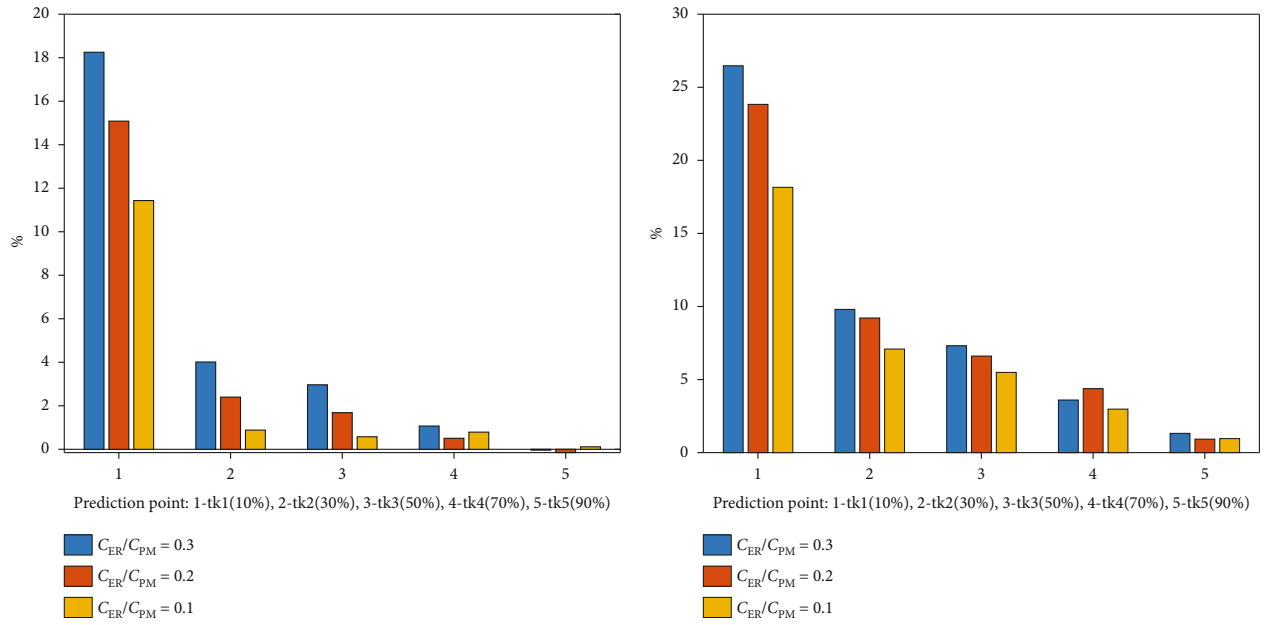

Figure 12: Maintenance evaluation index. (a) Average cost rate percentage with three maintenance ratios under 30 training-test set schemes. (b) Average maintenance interval percentage with three maintenance ratios under 30 training-test set schemes.

Table 6: The maintenance performance comparison of cost rate percentage R_η (%) between the BP and the combination BP-RBF-GRNN neural network model under three different maintenance cost ratios (C_{PM}/C_{ER}).

C_{PM}/C_{ER}	t_{k1}	t_{k2}	t_{k3}	t_{k4}	t_{k5}
0.5	15.92	17.14	15.28	7.42	1.86
0.4	14.31	15.62	12.28	5.73	1.35
0.3	12.61	14.40	9.34	3.80	0.91

Table 7: The maintenance performance comparison of cost rate percentage R_η (%) between the RBF and the combination BP-RBF-GRNN neural network model under three different maintenance cost ratios (C_{PM}/C_{ER}).

C_{PM}/C_{ER}	t_{k1}	t_{k2}	t_{k3}	t_{k4}	t_{k5}
0.5	0.26	0.24	0.27	0.20	0.17
0.4	0.14	0.20	0.17	0.18	0.12
0.3	0.09	0.10	0.10	0.10	0.12

Table 8: The maintenance performance comparison of cost rate percentage R_η (%) between the GRNN and the combination BP-RBF-GRNN neural network model under three different maintenance cost ratios (C_{PM}/C_{ER}).

C_{PM}/C_{ER}	t_{k1}	t_{k2}	t_{k3}	t_{k4}	t_{k5}
0.5	4.18	2.00	0.55	0.29	0.17
0.4	3.81	1.46	0.73	0.35	0.24
0.3	3.51	1.56	1.05	0.36	0.01

Table 9: The maintenance performance comparison of maintenance interval percentage $R_{T\text{opt}}$ (%) between the BP and the combination BP-RBF-GRNN neural network model under three different maintenance cost ratios (C_{PM}/C_{ER}).

C_{PM}/C_{ER}	t_{k1}	t_{k2}	t_{k3}	t_{k4}	t_{k5}
0.5	31.05	32.85	29.62	15.96	4.11
0.4	30.45	32.09	26.72	15.14	3.73
0.3	29.84	32.75	23.91	11.64	3.49

Table 10: The maintenance performance comparison of maintenance interval percentage $R_{T\text{opt}}$ (%) between the RBF and the combination BP-RBF-GRNN neural network model under three different maintenance cost ratios (C_{PM}/C_{ER}).

C_{PM}/C_{ER}	t_{k1}	t_{k2}	t_{k3}	t_{k4}	t_{k5}
0.5	1.57	2.08	2.22	1.47	0.64
0.4	1.32	1.78	1.31	1.39	0.50
0.3	1.00	1.22	1.23	1.65	0.38

Table 11: The maintenance performance comparison of maintenance interval percentage $R_{T\text{opt}}$ (%) between the GRNN and the combination BP-RBF-GRNN neural network model under three different maintenance cost ratios (C_{PM}/C_{ER}).

C_{PM}/C_{ER}	t_{k1}	t_{k2}	t_{k3}	t_{k4}	t_{k5}
0.5	9.47	5.72	2.38	1.86	0.90
0.4	9.99	5.54	3.11	1.46	1.21
0.3	9.89	5.75	4.77	1.83	0.51

Table 12: The prediction performance comparison of the BP, RBF, GRNN, and combination method.

Method	t_{k1}	t_{k2}	t_{k3}	t_{k4}	t_{k5}
BP	0.3101	0.3092	0.3139	0.2141	0.1907
RBF	0.0167	0.0175	0.0182	0.0177	0.0183
GRNN	0.1821	0.0358	0.0238	0.0165	0.0159
Combination BP-RBF-GRNN neural network model	0.0045	0.0049	0.0055	0.0055	0.0056

Table 13: The introduction of the experimental design scheme.

Experimental design scheme	Covariate simulation parameter
1st degeneration scenario	$\theta' \sim N(\mu_0, \sigma_0^2), \beta' \sim N(\mu_1', \sigma_1'), \varepsilon(t_i) - \varepsilon(t_{i-1}) \sim N(0.5 \times \mu_0, 0.5 \times \sigma^2)$
2nd degeneration scenario	$\theta' \sim N(\mu_0, \sigma_0^2), \beta' \sim N(\mu_1', \sigma_1'), \varepsilon(t_i) - \varepsilon(t_{i-1}) \sim N(1 \times \mu_0, 1 \times \sigma^2)$
3rd degeneration scenario	$\theta' \sim N(\mu_0, \sigma_0^2), \beta' \sim N(\mu_1', \sigma_1'), \varepsilon(t_i) - \varepsilon(t_{i-1}) \sim N(2 \times \mu_0, 2 \times \sigma^2)$

Table 14 is the prediction performance of the Bayesian parameter updating prediction model and combination BP-RBF-GRNN neural network model in RMSPE under three different degeneration scenarios. The result in Table 14 can be calculated by using the prediction error minuses that of the combination BP-RBF-GRNN neural network model, and the high value of RMSPE means the low prediction performance. As shown in Table 14, we can draw the conclusion that in every degeneration scenario, the prediction performance of the combination BP-RBF-GRNN neural network model from the early-stage to the mid-stage is more advantageous than those of the Bayesian parameter updating forecasting model.

Tables 15 and 16 are the maintenance performance of the Bayesian parameter updating prediction model and combination BP-RBF-GRNN neural network model in cost rate and maintenance under three different degeneration scenarios when $C_{PM}/C_{ER} = 0.3$, respectively. Table 15 represents the cost rate percentage, which uses the cost rate of the Bayesian parameter updating prediction model to be divided by that of the combination BP-RBF-GRNN neural network model. The value of the cost rate percentage is greater than 0, which means that the cost of the Bayesian parameter updating prediction model is higher than that of the combination BP-RBF-GRNN neural network model. And if the value of the cost rate percentage is high, the cost of the combination BP-RBF-GRNN neural network model will be low. As shown in Equation (26), Table 16 represents the maintenance interval percentage, which uses the maintenance interval of the combination BP-RBF-GRNN neural network model to be divided by that of the Bayesian parameter updating prediction model. The value of the maintenance interval percentage is greater than 0, which means that the maintenance performance of the combination BP-RBF-GRNN neural network model is higher than that of the Bayesian parameter updating prediction model. And if the value of the maintenance interval percentage is high, the maintenance performance of the combination BP-RBF-GRNN neural network model will be good. The high value

Table 14: The prediction performance difference of RMSPE (%) between the combination BP-RBF-GRNN neural network model and Bayesian parameter updating prediction model under different degeneration scenarios.

Experimental design scheme	t_{k1}	t_{k2}	t_{k3}	t_{k4}	t_{k5}
1st degeneration scenario	1.98	1.78	1.14	0.06	-0.06
2nd degeneration scenario	9.83	5.67	3.65	0.08	-0.07
3rd degeneration scenario	6.78	3.51	1.63	-0.09	-0.04

Table 15: The maintenance performance comparison of cost rate percentage R_η (%) between the combination BP-RBF-GRNN neural network model and Bayesian parameter updating prediction model when $C_{PM}/C_{ER} = 0.3$ under different degeneration scenarios.

Experimental design scheme	t_{k1}	t_{k2}	t_{k3}	t_{k4}	t_{k5}
1st degeneration scenario	16.45	8.43	3.39	0.54	0.22
2nd degeneration scenario	18.25	4.01	2.96	1.07	-0.04
3rd degeneration scenario	20.70	14.56	9.02	2.92	1.31

Table 16: The maintenance performance comparison of maintenance interval percentage $R_{T\text{opt}}$ (%) between the combination BP-RBF-GRNN neural network model and Bayesian parameter updating prediction model when $C_{PM}/C_{ER} = 0.3$ under different degeneration scenarios.

Experimental design scheme	t_{k1}	t_{k2}	t_{k3}	t_{k4}	t_{k5}
1st degeneration scenario	20.22	11.66	7.95	4.38	2.07
2nd degeneration scenario	26.47	9.80	7.32	3.60	1.32
3rd degeneration scenario	21.05	15.02	8.49	3.18	2.19

Table 17: Computational cost (second).

Bayesian parameter updating prediction model	Combination BP-RBF-GRNN neural network model
201.39	334.16

in Tables 15 and 16 means that the combination BP-RBF-GRNN neural network model has a better maintenance performance than that of the Bayesian parameter updating prediction model. As shown in Tables 15 and 16, we can draw the conclusion that in every degeneration scenario, the cost rate percentage and maintenance interval percentage of the combination BP-RBF-GRNN neural network model from the early-stage to the mid-stage are more advantageous than those of Bayesian parameter updating prediction model. The conclusion from Table 14 and Tables 15 and 16 can illustrate the fact that the improvement of accuracy will improve the maintenance efficiency.

5.3.4. Computational Cost. We use a laptop computer as a baseline device. Its specifications include an Intel Core i7-9750H processor with a base frequency of 2.60 GHz, equipped with 16 GB of RAM. The comparison of computational cost between the combination BP-RBF-GRNN neural network model and the Bayesian parameter updating prediction model is shown in Table 17. We calculated the cost of the first experiment (Figures 8–12), which includes the cost from five predicted points for two prediction models under 30 training-test set schemes. It can be clearly found that the computational cost of the combination BP-RBF-GRNN neural network model is not much higher than that of the Bayesian parameter updating prediction model. But the combination BP-RBF-GRNN neural network model has a better performance than the Bayesian parameter updating prediction model in degeneration prediction and maintenance. The explanation for the above result is as follows. The Bayesian parameter updating prediction model uses the prior distributions of model parameters to obtain that of the posterior distributions, and the Monte Carlo Simulation is used to simulate N degeneration scenarios to predict the degeneration process. However, the high degeneration scenario will lead to the high computational cost of the Bayesian parameter updating prediction model. In order to improve the accuracy of the degradation process, we simulated 10000 degradation scenarios at each predicted point under 30 training-test set schemes, which resulted in high computational cost. The combination BP-RBF-GRNN neural network model contains three prediction sub-models, namely, BP, RBF, and GRNN neural network. The BP and RBF neural networks adopt one hidden layer. One hidden layer normally does not cause high computational cost. Although the GRNN neural network uses two hidden layers, the weight of the whole neural network is equal to 1, which indicates that two adjacent layers can be connected without updating the weight, thus reducing the computational cost.

6. Conclusion

This paper puts forward a predictive maintenance optimization framework based on the proportional hazard model and BP-RBF-GRNN neural network model to improve the accuracy of degeneration prediction and reduce the maintenance cost to a certain extent. The main contribution can be illustrated in two aspects. Firstly, the combination forecasting method based on deep learning is rarely applied in degeneration prediction, which can improve the accuracy of degeneration. Therefore, the combination BP-RBF-GRNN neural network model based on deep learning is used to predict the degeneration prediction. Secondly, condition monitoring data may not directly reflect the degree of degeneration, life data and condition monitoring values must be considered comprehensively. Therefore, WPHM which considers both life data and condition monitoring values can be used to evaluate the hazard rate. We design two experiments to illustrate the advantage of combination BP-RBF-GRNN neural network model. For the first experiment, we compared the combination BP-RBF-GRNN neural network model to the Bayesian parameter updating prediction model in prediction performance and maintenance performance. The simulation results show that the combination BP-RBF-GRNN neural network model can effectively improve the accuracy of the thrust ball bearings degeneration process and reduce the maintenance cost percentage from early-stage to mid-stage than that of the Bayesian parameter updating prediction model. For the second experiment, we compared the combination BP-RBF-GRNN neural network model to other three single deep learning models in prediction performance and maintenance performance. The simulation results show that the combination BP-RBF-GRNN neural network model has advantages over other three single prediction sub-models in cost rate percentage and maintenance interval percentage from the early-stage to the mid-stage.

Data Availability

The data used to support the findings of this study are available from the corresponding author upon request.

Conflicts of Interest

The authors declare no conflict of interest.

Acknowledgments

This research was supported by the National Key Research and Development Program of China "Manufacturing Basic Technology and Key Components" key project (Grant No. 2021YFB2011200). This work was also supported by the National Natural Science Foundation of China (Grant No. 71501148).

References

[1] A. Patwardhan, A. K. Verma, and U. Kumar, "A survey on predictive maintenance through big data," in *Current Trends in Reliability, Availability, Maintainability and Safety*, pp. 437–445, Springer, 2016.

[2] L. Spendla, M. Kebisek, P. Tanuska, and L. Hrcka, "Concept of predictive maintenance of production systems in accordance with industry 4.0," in *2017 IEEE 15th International Symposium*

on Applied Machine Intelligence and Informatics (SAMI), Herl'any, Slovakia, 2017.

[3] N. Sakib and T. Wuest, "Challenges and opportunities of condition-based predictive maintenance: a review," *Procedia CIRP*, vol. 78, pp. 267–272, 2018.

[4] T. P. Carvalho, F. A. A. M. N. Soares, R. Vita, R. . P. Francisco, J. P. Basto, and S. G. S. Alcalá, "A systematic literature review of machine learning methods applied to predictive maintenance," *Computers & Industrial Engineering*, vol. 137, article 106024, 2019.

[5] H. D. Faria, J. Costa, and J. Olivas, "A review of monitoring methods for predictive maintenance of electric power transformers based on dissolved gas analysis," *Renewable and Sustainable Energy Reviews*, vol. 46, pp. 201–209, 2015.

[6] W. Zhe, W. Fei, and S. Shi, "Solar irradiance short-term prediction model based on BP neural network," *Energy Procedia*, vol. 12, pp. 488–494, 2011.

[7] Y. Zhao, J. Nan, F. Y. Cui, and L. Guo, "Water quality forecast through application of BP neural network at Yuqiao reservoir," *Journal of Zhejiang University-SCIENCE A*, vol. 8, no. 9, pp. 1482–1487, 2007.

[8] H. Bendu, B. B. V. Deepak, and S. Murugan, "Application of GRNN for the prediction of performance and exhaust emissions in HCCI engine using ethanol," *Energy Conversion and Management*, vol. 122, pp. 165–173, 2016.

[9] I. Ladlani, L. Houichi, L. Djemili, S. Heddam, and K. Belouz, "Modeling daily reference evapotranspiration (ET0) in the north of Algeria using generalized regression neural networks (GRNN) and radial basis function neural networks (RBFNN): a comparative study," *Meteorology and Atmospheric Physics*, vol. 118, no. 3-4, pp. 163–178, 2012.

[10] M. Kamiński and M. Solecka, "Optimization of the truss-type structures using the generalized perturbation- based Stochastic Finite Element Method," *Finite Elements in Analysis and Design*, vol. 63, pp. 69–79, 2013.

[11] S. Bressi, J. Santos, and M. Losa, "Optimization of maintenance strategies for railway track-bed considering probabilistic degradation models and different reliability levels," *Reliability Engineering & System Safety*, vol. 207, article 107359, 2021.

[12] H. Dui, C. Zhang, G. Bai, and L. Chen, "Mission reliability modeling of UAV swarm and its structure optimization based on importance measure," *Reliability Engineering & System Safety*, vol. 215, article 107879, 2021.

[13] B. Yin, Y. Li, S. Miao, Y. Lin, and H. Zhao, "An economy and reliability co-optimization planning method of adiabatic compressed air energy storage for urban integrated energy system," *Journal of Energy Storage*, vol. 40, article 102691, 2021.

[14] Z. Han, L. Tian, and L. Cheng, "A deducing-based reliability optimization for electrical equipment with constant failure rate components duration their mission profile," *Reliability Engineering & System Safety*, vol. 212, no. 2, article 107575, 2021.

[15] M. Leimeister and A. Kolios, "A review of reliability-based methods for risk analysis and their application in the offshore wind industry," *Renewable and Sustainable Energy Reviews*, vol. 91, pp. 1065–1076, 2018.

[16] S. Wu, N. Gebraeel, M. Lawley, and Y. Yih, "A neural network integrated decision support system for condition-based optimal predictive maintenance policy," *IEEE Transactions on Systems, Man, and Cybernetics - Part A. Systems and Humans*, vol. 37, no. 2, pp. 226–236, 2007.

[17] A. C. Mendes and N. Fard, "Accelerated failure time models comparison to the proportional hazard model for time-dependent covariates with recurring events," *International Journal of Reliability, Quality and Safety Engineering*, vol. 21, no. 2, article 1450010, 2014.

[18] N. Gorjian, L. Ma, M. Mittinty, P. Yarlagadda, and Y. Sun, "A review on reliability models with covariates," in *Engineering Asset Lifecycle Management*, pp. 385–397, Springer, 2010.

[19] Z. Xu, "Statistical modeling and predictions based on field data and," *Dynamic Covariates*, 2 3, 2014.

[20] N. G. Wang, X. W. Zhu, and J. Zhang, "License plate segmentation and recognition of Chinese vehicle based on BPNN," in *2016 12th International Conference on Computational Intelligence and Security (CIS)*, Wuxi, China, 2016.

[21] Y. Dai, J. Guo, L. Yang, and W. You, "A new approach of intelligent physical health evaluation based on GRNN and BPNN by using a wearable smart bracelet system," *Procedia Computer Science*, vol. 147, pp. 519–527, 2019.

[22] J. Li, J.-h. Cheng, J.-y. Shi, and F. Huang, "Brief introduction of back propagation (BP) neural network algorithm and its improvement," in *Advances in Computer Science and Information Engineering*, pp. 553–558, Springer, 2012.

[23] B. Wang, X. Gu, L. Ma, and S. Yan, "Temperature error correction based on BP neural network in meteorological wireless sensor network," *International Conference on Cloud Computing & Security*, vol. 23, no. 4, p. 265, 2017.

[24] M. Maarouf, A. Sosa, B. Galván et al., "The role of artificial neural networks in evolutionary optimisation. A review," in *Advances in Evolutionary and Deterministic Methods for Design, Optimization and Control in Engineering and Sciences*, vol. 36, pp. 59–76, Springer International Publishing, 2015.

[25] T. K. Leong, P. Saratchandran, and N. Sundararajan, "Real-time performance evaluation of the minimal radial basis function network for identification of time varying nonlinear systems," *Computers and Electrical Engineering*, vol. 28, no. 2, pp. 103–117, 2002.

[26] D. F. Specht, "A general regression neural network," *IEEE Transactions on Neural Networks*, vol. 2, no. 6, pp. 568–576, 1991.

[27] W. Li, X. Yang, H. Li, X. Yang, H. Li, and L. Su, "Hybrid forecasting approach based on GRNN neural network and SVR machine for electricity demand forecasting," *Energies*, vol. 10, no. 1, p. 44, 2017.

[28] S. Yin, L. Liu, and J. Hou, "A multivariate statistical combination forecasting method for product quality evaluation," *Information Sciences*, vol. 355-356, pp. 229–236, 2016.

[29] A. R. Aladro-Gonzalvo, G. A. Araya-Vargas, M. Machado-Díaz, and W. Salazar-Rojas, "Pilates-based exercise for persistent, non-specific low back pain and associated functional disability: A meta-analysis with meta-regression," *Journal of Bodywork and Movement Therapies*, vol. 17, no. 1, pp. 125–136, 2013.

[30] Q. Zhang, C. Hua, and G. Xu, "A mixture Weibull proportional hazard model for mechanical system failure prediction utilising lifetime and monitoring data," *Mechanical Systems and Signal Processing*, vol. 43, no. 1-2, pp. 103–112, 2014.

[31] H. K. Ghritlahre and R. K. Prasad, "Investigation of thermal performance of unidirectional flow porous bed solar air heater using MLP, GRNN, and RBF models of ANN technique," *Thermal Science and Engineering Progress*, vol. 6, pp. 226–235, 2018.

[32] B. De Jonge, W. Klingenberg, and R. Teunter, "Optimum maintenance strategy under uncertainty in the lifetime distribution," *Reliability Engineering & System Safety*, vol. 133, pp. 59–67, 2015.

[33] N. Z. Gebraeel, M. A. Lawley, R. Li, and J. K. Ryan, "Residual-life distributions from component degradation signals: a Bayesian approach," *IIE Transactions*, vol. 37, no. 6, pp. 543–557, 2005.

[34] G. Q. Tong and X. B. Qian, "An extended predictive maintenance model under covariate distribution parameters with uncertainty," in *Proceedings of the RICAI 2020.2020 2nd International Conference on Robotics, Intelligent Control and Artificial Intelligence*, Shanghai, China, 2020.

[35] A. H. Elwany, N. Gebraeel, and L. M. Maillart, "Structured replacement policies for components with complex degradation processes and dedicated sensors," *Operations Research*, vol. 59, no. 3, pp. 684–695, 2011.